Microsolvation in superfluid helium droplets studied by the electronic spectra of six porphyrin derivatives and one chlorine compound

R. Riechers, D. Pentlehner, and A. Slenczka

Articles you may be interested in

Helium induced fine structure in the electronic spectra of anthracene derivatives doped into superfluid helium nanodroplets
J. Chem. Phys. **142**, 014311 (2015); 10.1063/1.4904899

Line broadening in electronic spectra of anthracene derivatives inside superfluid helium nanodroplets
J. Chem. Phys. **133**, 114505 (2010); 10.1063/1.3479583

Near-infrared spectroscopy of ethylene and ethylene dimer in superfluid helium droplets
J. Chem. Phys. **122**, 104307 (2005); 10.1063/1.1854630

Fine structure of the (S 1 ←S 0) band origins of phthalocyanine molecules in helium droplets
J. Chem. Phys. **121**, 9396 (2004); 10.1063/1.1804945

Quantum solvation of phthalocyanine in superfluid helium droplets
J. Chem. Phys. **120**, 5064 (2004); 10.1063/1.1647536

Microsolvation in superfluid helium droplets studied by the electronic spectra of six porphyrin derivatives and one chlorine compound

R. Riechers,[a)] D. Pentlehner,[b)] and A. Slenczka[c)]
Institut für Physikalische und Theoretische Chemie, Universität Regensburg, 93040 Regensburg, Germany

After almost two decades of high resolution molecular spectroscopy in superfluid helium droplets, the understanding of microsolvation is still the subject of intense experimental and theoretical research. According to the published spectroscopic work including microwave, infrared, and electronic spectroscopy, the latter appears to be particularly promising to study microsolvation because of the appearance of pure molecular transitions and spectrally separated phonon wings. Instead of studying the very details of the influence of the helium environment for one particular dopant molecule as previously done for phthalocyanine, the present study compares electronic spectra of a series of non-polar porphyrin derivatives when doped into helium droplets consisting of 10^4–10^5 helium atoms. Thereby, we focus on the helium-induced fine structure, as revealed most clearly at the corresponding electronic origin. The interpretation and the assignment of particular features obtained in the fluorescence excitation spectra are based on additional investigations of dispersed emission spectra and of the saturation behavior. Besides many dopant-specific results, the experimental study provides strong evidence for a particular triple peak feature representing the characteristic signature of helium solvation for all seven related dopant species. © *2013 AIP Publishing LLC.*
[http://dx.doi.org/10.1063/1.4811199]

I. INTRODUCTION

Microsolvation of molecules in superfluid helium droplets can be studied by means of high resolution spectroscopy and, if available, by comparison with corresponding experimental data from the gas phase. The first rotationally resolved infrared spectrum showing the ν_6 mode of SF_6 revealed that SF_6 resides inside the helium droplet and forms a complex with 8 helium atoms, one attached to each of the 8 faces of the dopant molecule.[1] Our work concentrates on electronic spectroscopy of molecules in helium droplets, and originally aimed to investigate photochemical processes of molecules at low temperature.[2] Surprising line broadening of electronic transitions taught us that unimolecular processes such as excited state intramolecular proton transfer (ESIPT) are greatly influenced by the helium environment.[3] As deduced from a systematic investigation including photochemically inactive species, the changing electron density distribution appeared to be a key quantity responsible for the spectral signature of solvation of molecules in helium droplets.[3–7] Besides a solvent shift, which is generally observed with any kind of solvent, one of the first helium-induced features observed in electronic spectra was the double peak splitting of all zero phonon lines (ZPL) of tetracene.[8, 9] Much effort has been put into the investigation of the details of this particular double peak signal, commonly named the α and the β lines.[10–12] With greatly improved spectral resolution, a pronounced fine structure has been recorded exclusively for the β line.[13] Thereby, the comparison not only with the corresponding gas phase data, but also with different but related dopant species, helped to identify and interpret the helium-induced spectroscopic features. For example, pentacene was found to exhibit a single peaked ZPL,[9] which, however, shows precisely the same fine structure as the β line of tetracene[13] when recorded under high resolution conditions. High resolution was achieved by using a cw single-mode ring dye laser instead of a pulsed multi-mode dye laser. Not only the difference in the bandwidth (about four orders of magnitude), but also the different intensity or photon flux (up to 6 orders of magnitude), improves the spectral resolution. Besides the challenges in dealing with electronically excited states, electronic spectroscopy has the advantage of providing pure molecular transitions (ZPL) and phonon wings (PW, which are excitations of the helium environment coupled to the molecular transitions) often spectrally well separated.[14–16] Narrow bandwidth in combination with low photon flux allows the resolution of the details of a ZPL, whereas high photon flux provides access to the PW. While most of the helium-induced spectroscopic features can be explained empirically, quantitative simulation is a challenge to be solved. This lack reveals the complexity of microsolvation in helium droplets and, despite the amount of experimental data, probably a lack of consistency in the experimental work. As clearly shown by the example of tetracene,[13] data with the highest spectral resolution are needed. Moreover, an interpretation profits greatly from comparison with related dopant species. In the case of tetracene, the β line has a different meaning and was proposed

---

a)Present address: Zeiss Laser Optics GmbH, Oberkochen, Germany.
b)Present address: Department of Chemistry, University of Aarhus, Aarhus, Denmark.
c)Author to whom correspondence should be addressed. Electronic mail: alkwin.slenczka@chemie.uni-regensburg.de

138, 244303-1

to reflect the interaction with vortices in the helium droplet.[13] This additional information is certainly very important for the theoretical approach.[17–19]

The present paper provides a comparative investigation of seven different but related molecular species with the aim of identifying the essential spectroscopic features of microsolvation for these compounds in superfluid helium droplets. The spectral resolution and the photon flux are essential parameters whereas the droplet size, kept between 10^4 and 10^5 helium atoms, covers a regime of negligible size effects. The dopant species include six porphyrin derivatives shown in Fig. 1, namely, free base porphyrin (henceforth addressed as porphyrin), 5,15-diphenylporphyrin (DPP), 5,10,15,20-tetraphenylporphyrin (TPP), 5,10,15,20-tetramethylporphyrin (TMP), 5,10,15,20-tetrapropylporphyrin (TPrP), 2,7,12,17-tetraethyl-3,8,13,18-tetramethylporphyrin also called etioporphyrin I (Etio), and finally 5,10,15,20-tetraphenylchlorine (TPC) not shown in Fig. 1. After an explanation of the experimental setup, the spectroscopic data will be presented. The discussion of the experimental data aims to identify similarities and dissimilarities in the spectra of the seven molecular compounds with particular emphasis on their electronic origins. Thereby, we
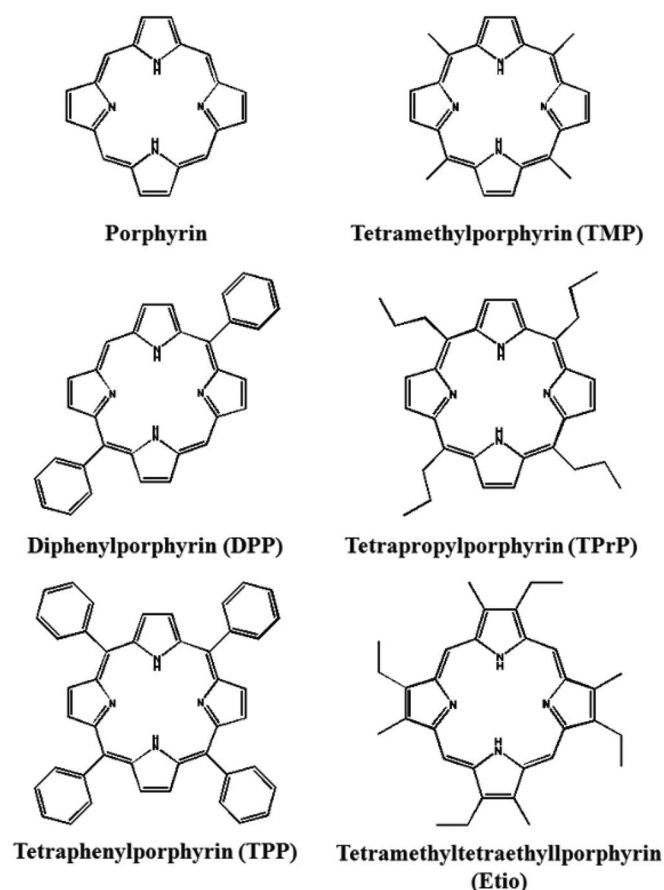

FIG. 1. Pophyrin derivatives investigated by means of electronic spectroscopy. The substituted porphyrins are not planar and therefore exhibit configurational variants with respect to bending and/or torsional angles of the substituents. The synthesis of TPP is known to be accompanied by minor contributions of TPC (not shown) with one of the four pyrrole-rings replaced by a pyrroline-ring.

assign essential spectral features which may guide theoretical activities on microsolvation in superfluid helium droplets.

II. EXPERIMENT

Two experimental setups have been used for recording electronic spectra of porphyrins in helium droplets which will be addressed as the *cw setup* and the *pulsed setup*. The denomination relates to both, the helium droplet source and the frequency-tunable dye laser system used in the two setups. The cw setup was operated with a high resolution (10^{-5} cm^{-1} bandwidth) single-mode ring dye laser (Coherent 899-21 pumped by an Ar$^+$-ion laser Sabre-R 25) while the pulsed setup was equipped with a pulsed dye laser (Lambda Physics Scanmate 2) with a bandwidth of about 0.2 cm^{-1} pumped by a Nd:YAG laser. Both vacuum machines consisted of two differentially pumped vacuum chambers. In the first chamber, the helium droplet source was operated and in the second the doping and the fluorescence detection took place. The cw setup was equipped with a continuous flow helium droplet source as developed in Göttingen.[20] The corresponding vacuum chamber was pumped by an oil diffusion pump (Leybold DI6000) backed by a roots blower (Leybold RUWAC 250) and a mechanical pump (Leybold). Passing through a conically shaped skimmer (Beam Dynamics) with 2 mm diameter situated about 1.8 cm behind the nozzle, the droplet beam entered the detection chamber. About 13 cm behind the nozzle, the droplet beam passed through a pick-up unit, consisting of a resistively heated oven with 3 mm openings on the droplet beam axis, which was shielded by a liquid-nitrogen cooled brass tubing. At an additional distance of 8 cm, the droplet beam was intersected by the cw-laser beam perpendicularly. The fluorescence was collected perpendicularly to the plane of laser and droplet beam by a collecting lens (f-number = 2.4). Two detector schemes were installed for recording either fluorescence excitation spectra or dispersed emission spectra. In the first case, the fluorescence was imaged onto the photocathode of a photomultiplier tube (PMT) (Hamamatsu R943-2), shielded from laser stray light by an appropriate cut-off filter, whose signal was amplified (SR445) and fed into a computer-controlled gated photon counter (SR400). Data acquisition and laser frequency stepping was synchronized via hand shaking between the photon counter and the frequency tuning electronics of the dye laser. In the second case, the fluorescence was imaged into the entrance slit of a spectrograph, equipped with a charge coupled device (CCD) camera (ANDOR DU401-BV) with a 256 × 1024 pixel diode array which was operated in full vertical binning mode providing spectra of 1024 data points. The spectral resolution in the red spectral range was 0.7 cm^{-1} per pixel at optimum conditions. Dispersed emission spectra have been recorded exclusively with the cw setup. The software of the camera was capable of recognizing signals from cosmic radiations which were eliminated.

The pulsed setup consisted of a pulsed dye laser used in combination with a pulsed droplet source. The droplet source was based on the high repetition Even-Lavie valve[21] modified for cryogenic operation, as described in Ref. 22. The

corresponding vacuum chamber was evacuated with a turbo pump (Balzers 2000), backed by a roots blower and a mechanical pump. The pulsed droplet beam entered the detection chamber through a home-made conical skimmer with an opening diameter of 6 mm. The doping unit and the detection unit were identical to those of the cw setup. The output of the PMT was amplified (ORTEC VT120) and fed into a gated boxcar averager (SR250). Besides the difference in the duty cycle, the spectral resolution and the photon flux of the excitation laser and the average droplet size were the major differences of both setups. A bandwidth of about 10^{-5} cm^{-1} and a photon rate of about 10^{17} photons per second for the cw-laser beam contrasts to a bandwidth of 0.2 cm^{-1} and a photon rate of 10^{25} s^{-1} for the pulsed laser beam. Assuming identical focal spot sizes of both laser systems, the spectral photon flux density differed by almost 4 orders of magnitude. The high photon flux of the pulsed setup accomplished fast recording of fluorescence excitation spectra of the porphyrin derivatives which are characterized by rather small oscillator strengths and small fluorescence quantum yields. After identifying the electronic origin and vibronic transitions, these resonances were recorded with the high spectral resolution of the cw setup, which was necessary to fully resolve the fine structures in the spectra. The cw setup was operated at a stagnation pressure of 20 bars and a nozzle temperature of about 11 K generating droplets of an average size of roughly 20 000 helium atoms.[23] The pulsed setup was operated at a stagnation pressure of 80 bars and a nozzle temperature of roughly 22 K providing droplets of an average size in the order of 10^5 helium atoms.[22] All dopant species have been sublimated in a resistively heated oven at temperatures which provided vapor pressures optimized for single molecule doping of the helium droplets. As will be discussed below, several of the samples came with moderate purity which was confirmed by chromatography. The spectral features discussed in this paper are all insensitive to the droplet size in the range from 10^4 to 10^5 helium atoms.

III. EXPERIMENTAL RESULTS

Recording fluorescence excitation spectra of porphyrins is a challenge because of the small oscillator strength in the order of f = 10^{-2} for the S$_0$–S$_1$ transition in combination with a small fluorescence quantum yield caused by a high triplet quantum yield.[24–28] It is even more challenging to record dispersed emission spectra where only a fraction of the weak fluorescence is dispersed over the 1024 × 256 pixels of a CCD chip. Therefore, the signal to noise level was much lower as compared to the phthalocyanines.

A. Porphyrin in helium droplets

The fluorescence excitation spectrum of porphyrin, measured with the cw setup over a frequency range of roughly 1000 cm^{-1}, is shown in the top panel of Fig. 2. Besides the electronic origin which peaks at 16 312.4 cm^{-1} and exhibits a helium solvent shift of only 8 cm^{-1} to the red,[29] vibronic transitions are nicely resolved. Throughout, the vibronic tran-
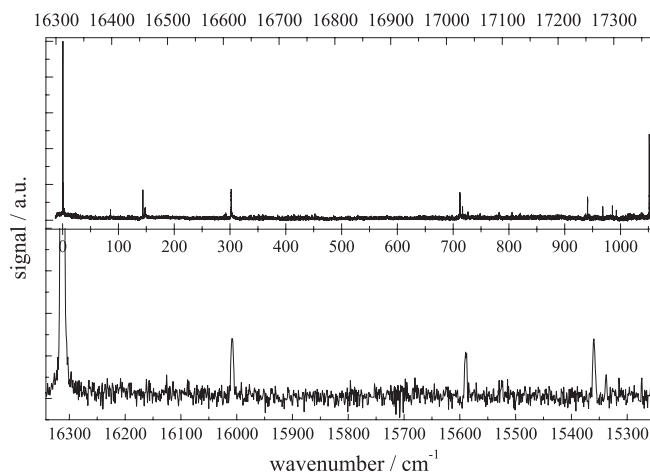

FIG. 2. (Top panel) Fluorescence excitation spectrum of porphyrin in helium droplets. (Bottom panel) Dispersed emission spectrum of porphyrin in helium droplets with inverted wavenumber scale. The center abscissa is scaled to the common origin at 16 312.4 cm^{-1} and allows for directly reading of vibrational wavenumbers.

sitions appear as sharp peaks with full width at half maximum of less than 1 cm^{-1}. The helium droplet spectrum shows only those transitions which have been assigned to fundamental modes in the gas phase while all others are missing.[29] The dispersed emission spectrum recorded upon excitation at the electronic origin is plotted in the bottom panel of Fig. 2 with an inverted wavenumber scale. The two spectra in Fig. 2 reveal nearly identical vibrational frequencies in the S$_0$ and the S$_1$ states. Differences in the intensity profile of both spectra are partly the result of different spectral resolution. In addition, the dispersed emission reflects the distribution of the transition probability while the intensity in the excitation spectrum is modified additionally by the state-specific fluorescence quantum yield, the spectral intensity profile of the laser, and by saturation in particular at the electronic origin. Finally, in the dispersed emission spectrum some of the vibronic transitions may be close to or even below the detection limit given by the noise level of the CCD camera. The resonance frequencies recorded over a large frequency range reveal properties of the dopant molecule. In the present case, the absence of vibrational progressions and the similarity of the wavenumber pattern of the two spectra in Fig. 2 reveal almost identical nuclear configuration and binding conditions for the S$_0$ and S$_1$ state of porphyrin. Since this paper is on microsolvation, we concentrate on spectral features that are caused by the interaction between dopant and helium droplet. Those are reflected by the fine structure of individual transitions recorded in the fluorescence excitation spectrum.

The fine structure at the electronic origin of the fluorescence excitation spectrum shown in the top panel of Fig. 3 has been reported long ago.[9] The same spectral section of only 6 cm^{-1} recorded with the cw setup (bottom panel of Fig. 3) reveals clearly a single sharp resonance followed by two weak but similarly sharp peaks. They are shifted by 0.4 and 0.7 cm^{-1} to the blue with a peak intensity of 19% and 12% of the first intense peak, respectively. This fine structure has not been reported in the gas phase. The frequency shift and the intensity pattern fit neither to normal mode
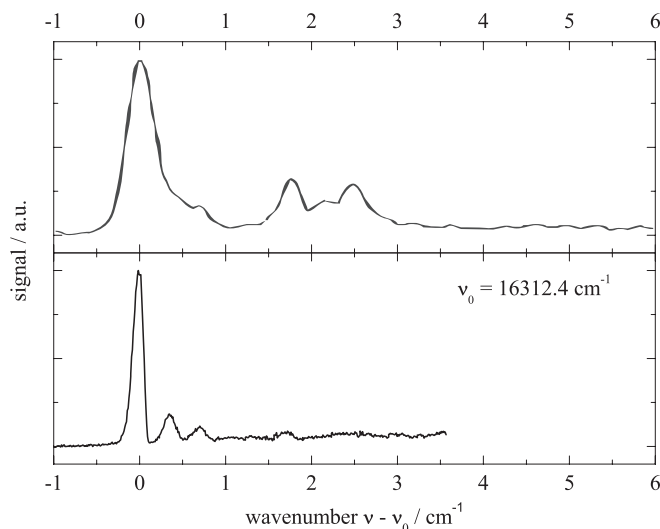
FIG. 3. Electronic origin of the fluorescence excitation spectrum of porphyrin in helium droplets recorded with a pulsed laser system (top panel) reproduced from Ref. 9 and with the cw setup (bottom panel).
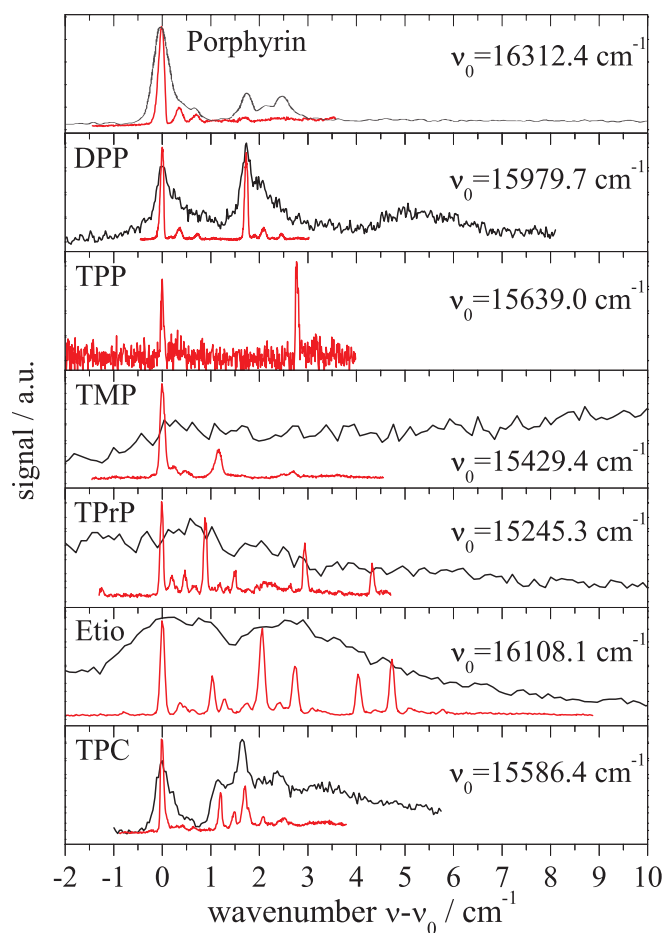

FIG. 4. Electronic origins of porphyrin derivatives in helium droplets as indicated. Each panel shows the spectrum recorded with the cw setup (red line) and the pulsed setup (black line). The wavenumber is counted from the corresponding origin whose absolute value is given in each panel.

frequencies of porphyrin nor to isomeric compounds with one ^{13}C isotope. The fine structure was not resolved in helium droplets when using the high power pulsed dye laser system in combination with a continuous droplet source[9,32] (cf. top panel of Fig. 3). However, the asymmetric line shape, recorded with severe saturation, can be reproduced by the triple peak feature convoluted with a line broadening function. Obviously, the intensity distribution within the triple peak feature does not change with the photon flux of the excitation laser which differs by roughly 4 orders of magnitude for the two experiments. Evidently, the three peaks exhibit identical oscillator strengths. In addition, the dispersed emission upon excitation at the first most intense peak coincides with the excitation frequency. Therefore, the entire triple peak structure fulfills the criteria of a ZPL. At a drastically increased photon flux as provided by the pulsed laser, an additional sharply structured signal could be recorded whose peaks are shifted by 1.8, 2.2, and 2.5 cm^{-1} with respect to the electronic origin[9] (cf. top panel Fig. 3). At the low photon flux of the cw-laser, only the first of these peaks at 1.8 cm^{-1} is visible. Obviously, beyond 1 cm^{-1} all the signal exhibits a smaller oscillator strength than the triple peak feature which is indicative for a PW. So far, our assignment is in line with previous work on porphyrin (cf. Ref. 9). The same triple peak feature appeared at vibronic transitions, in some cases with significantly increased line width, caused by the reduced lifetime of vibrationally excited states.

In order to evaluate the meaning of the triple peak ZPL observed for porphyrin in helium droplets, additional spectra of substituted porphyrin compounds have been investigated. High resolution fluorescence excitation spectra have been measured in helium droplets for the non-polar porphyrin derivatives listed in Fig. 1. Seven spectra are plotted in Fig. 4 with a common wavenumber axis scaled to the corresponding electronic origin. Each panel is labeled by the corresponding dopant species and the absolute wavenumber of the electronic origin. Moreover, each panel shows two spectra,

one measured with the cw setup (red line) and the other with the pulsed setup (black line). As discussed for porphyrin, the first spectrum reveals the fine structure of the ZPL whereas high photon flux is required for recording the PW. The top panel repeats the spectrum of porphyrin serving as master.

B. DPP in helium droplets

The second panel shows the electronic origin of DPP at 15 979.7 cm^{-1}. Obviously, double phenylation causes a redshift of 332.7 cm^{-1}. A triple peak fine structure can be recognized almost identical to the top panel. In contrast to porphyrin, this whole feature repeats shifted by 1.8 cm^{-1} to the blue. Using the pulsed setup with high photon flux, the fine structure shows saturation broadening for both triple peak features (black line). As for porphyrin, the saturated signal (black) reflects the fully resolved fine structure (red) after convolution with a line broadening function. The entire signal up to about 2.5 cm^{-1} shows identical oscillator strength and is therefore assigned to ZPLs. Only when using the pulsed setup, a broad signal shows up beyond 4 cm^{-1} excess energy. This signal shows the typical properties of a PW such as a significantly reduced oscillator strength and a blueshift of a few cm^{-1}.[9]

C. TPP in helium droplets

The third panel in Fig. 4 shows the fluorescence excitation spectrum of TPP with the origin at $15\,639.0$ cm^{-1}. This very weak signal could only be observed with the cw setup. When using the pulsed setup it was masked by a broad PW of a different species which will be discussed below. Fourfold phenylation causes a redshift of 673.4 cm^{-1}, almost twice as large as double phenylation. The spectrum reveals a doublet similar to DPP, however, with an increased gap of 2.8 cm^{-1}. Despite the low signal to noise ratio, both peaks seem to be accompanied by additional weak signals to the blue, which we identify as the low intensity part of the triple peak feature recorded for porphyrin and DPP. Unfortunately, the intensities expected for vibronic transitions accompanying this electronic origin are below the signal-to-noise limit. The same holds for vibronic transitions in the dispersed emission spectrum. Nevertheless, the assignment to an electronic origin is safely confirmed by the emission which was coincident with the corresponding excitation.

D. TMP, TPrP, and Etio in helium droplets

In addition to the phenylated porphyrin derivatives, electronic spectra of TMP, TPrP, and Etio have been recorded and are plotted in the following three panels of Fig. 4, as indicated. The corresponding electronic origins recorded with the cw setup (red lines) show several very sharp peaks. When recorded with the pulsed setup (black line), these features are not resolved because of severe saturation broadening and intense overlapping PWs. For all these three porphyrin compounds, the intensity distribution within the first 1 cm^{-1} is reminiscent of the triple peak feature of porphyrin. As to be expected, the spectral shape shows dopant specific modifications of both, the frequency position and the intensity level. With increasing size or number of the substituents, an increasing number of sharp peaks are recorded further to the blue. While TMP shows two additional peaks shifted by 1.1 and 2.7 cm^{-1}, TPrP shows four at 0.9, 1.5, 2.9, and 4.3 cm^{-1} and Etio even 5 at 1.0, 2.0, 2.7, 4.1, and 4.7 cm^{-1}. Again, dispersed emission spectra and saturation behavior reveal additional information on the nature of these signals. In the case of TMP, the emission upon excitation at the peak at 1.1 cm^{-1} was coincident to the emission upon excitation at the origin. The redshifted emission reveals either dissipation of excess excitation energy, which would speak for a PW, or for the relaxation of a metastable configuration of the excited dopant species, both prior to radiative decay. The particular spectral shape, reflecting largely the triple peak feature, speaks for metastable dopant species and, thus, favors an assignment to a ZPL. It should be mentioned that the experimental investigation cannot differentiate between the possibility of different intra-molecular configurations concerning the methyl moieties and different inter-molecular configurations concerning the structure of a helium solvation layer.

The spectrum of TPrP shows a rich fine structure which extends over about 20 cm^{-1} which will be discussed in a forthcoming paper. Here, we concentrate on a small spectral section shown in Fig. 4 which includes the electronic origin.

The intense peak shifted by 0.9 cm^{-1} to the blue of the origin exhibits the same triple peak fine structure as recorded at the origin. Similarly, the following three signals at 1.5, 2.9, and 4.3 cm^{-1} can be recognized as the leading intense peak of a triple peak feature. Similar as for TMP, TPrP may exhibit isomeric complexes which differ in the orientation of the propyl substituent and/or in the configuration of a helium solvation layer. In both cases, all peaks of the red spectra are interpreted as ZPLs.

Also for Etio the 5 sharp and intense peaks within the first 5 cm^{-1} are all accompanied to the blue by very weak signals and, therefore, can be seen as the leading peak of 5 triple peak features. For the six intense peaks including the origin, the first (origin), the third, and the 5th with equidistant gaps of 2 cm^{-1} exhibit the same emission spectrum whose origin coincides with the first peak. Similarly, the second, the 4th ($\Delta\bar{\nu} = 1.7$ cm^{-1}), and the 6th ($\Delta\bar{\nu} = 2.0$ cm^{-1}) exhibit a common emission spectrum whose origin coincides with the second peak. Most likely these 6 peaks can be attributed to isomeric configurations of Etio which differ either in the orientation of the substituents and/or in the configuration of the helium solvation layer and, thus, are all ZPLs. We need to note, that an alternative assignment of the 5 blueshifted peaks to a PW of the helium solvation layer cannot be strictly excluded. Nevertheless, the saturated spectrum of Etio shown as the black line in the bottom panel of Fig. 4 reveals very much the convolution of the corresponding high resolution spectrum (red line) with a line broadening function. This reveals a rather homogeneous oscillator strength throughout the spectrum and, thus, speaks for an assignment to ZPLs.

E. Unknown impurities and TPC in helium droplets

By using the cw setup for the sample of TMP, a second electronic origin has been identified at $15\,045.8$ cm^{-1}, as confirmed by the corresponding dispersed emission spectrum. At high laser intensities as provided by the pulsed setup, the signal of the corresponding series of vibronic transitions dominates over the true signal of TMP. The fine structure shown in Fig. 5 consists of a series of more than 10 equidistant peaks within the first 3–4 cm^{-1} which merge into a rather continuous signal extending over more than 50 cm^{-1}. According to the different saturation behaviors of the structured and continuous section, the latter is assigned to the PW. Since this spectral shape has no relation to the triple peak feature recorded for all the other porphyrin derivatives, this origin can only be attributed to some unknown impurity. A chromatographic analysis confirmed the contamination of the TMP sample by a second species. According to the corresponding chromatogram, the TPrP sample was contaminated with at least 5 additional species. Thus, the fluorescence excitation spectrum showed signals from TPrP and additional contributions from impurities. The signal of TPrP was identified by sorting all transitions with identical fine structure. Among the different groups, the one assigned to TPrP reflects the closest similarity to the vibrational fine structure of porphyrin.

Finally, the last panel in Fig. 4 shows the fluorescence excitation spectrum of TPC. This spectrum was recorded upon
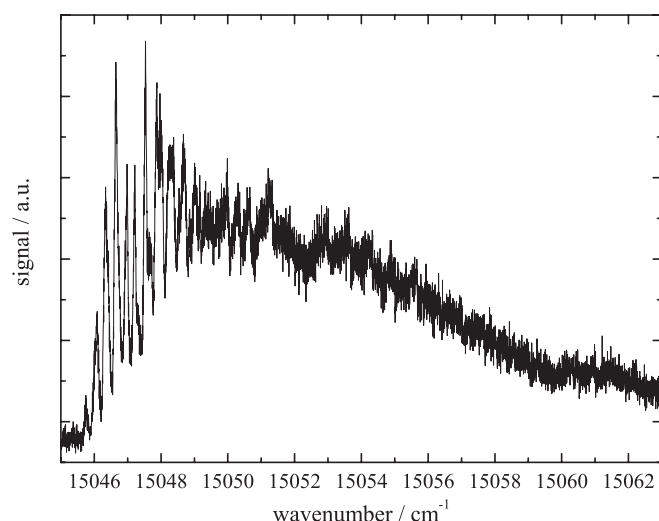
FIG. 5. A second origin identified in the fluorescence excitation spectrum of a TMP sample recorded with the cw setup. The corresponding molecular species could not be identified.

doping with the same sample used to record the TPP spectrum. The first peak at 15 586.4 cm^{-1} represents the electronic origin as revealed by coincident dispersed emission. It is shifted by an additional 52.4 cm^{-1} to the red so that the corresponding vibronic transitions and PWs overlap with the spectrum of TPP. Since it is well known that chlorines are a byproduct of the synthesis of porphyrins, we recorded the corresponding fluorescence excitation spectrum of a commercial sample of TPC. Using the pulsed setup, the spectra of both samples recorded over a range of roughly 700 cm^{-1} were identical. Figure 6 shows the fluorescence excitation spectrum of the TPC sample together with the dispersed emission spectrum upon excitation at the electronic origin. For TPC, the oscillator strength and fluorescence quantum yield are known to be much larger than for the corresponding porphyrin derivative.[24–28] Under these conditions, the fluorescence of a minor contamination with TPP could not be detected from the TPC sample while the fluorescence of a minor contami-

nation with TPC can even dominate the spectrum of a TPP sample. Further evidence for the contamination of the TPP sample with TPC was provided by the chromatograms which revealed the same two species for both samples, however, with almost inverted abundance.

Figure 6 reveals that the vibrational frequencies of TPC which can be read from the center abscissa are almost identical in S$_0$ (lower panel) and S$_1$ (upper panel). As the porphyrins, TPC is a rather rigid molecule with almost identical nuclear configuration and force constants in the S$_0$ and the S$_1$ states. Most clearly for the electronic origin of the fluorescence excitation spectrum but also for the vibronic transitions, an additional spectrally broad signal extends to the blue with maxima at additional 26 cm^{-1} and 60 cm^{-1}. Since this part of the signal was almost absent for the low photon flux of the cw setup, it has a very small oscillator strength which, together with the spectrally broad shape, provides evidence for an assignment to a PW. The progression of a low energy torsional mode observed in the corresponding gas phase experiment with peaks at additional 18, 40, and 61 cm^{-1}[30,31] does not fit to the signal observed in helium droplets. In the dispersed emission spectrum, the corresponding signal at the origin shows the same spectral shape as in the excitation (cf. Fig. 6). In contrast, the first vibronic transition is accompanied by two tiny and sharp peaks, shifted by 21 ± 2 and 43 ± 2 cm^{-1} to the red. These tiny peaks fit surprisingly well to a hot band of a torsional mode identified in the gas phase fluorescence excitation spectrum with a redshift of 22 ± 2 cm^{-1} with respect to the electronic origin.[30]

As is clearly visible in Fig. 7, the fluorescence excitation spectrum of the electronic origin of TPC shows additional spectral features to the blue. For the cw setup (red and black lines), the line width of the leading intense peak shrinks to only 0.05 cm^{-1}. Within the first 1 cm^{-1} to the blue, additional weak features are observed. Together with the leading peak it reminds of the triple peak feature identified for the porphyrins, albeit modified in the spectral shape. Further to the blue, a fine structure is recorded with peaks at 1.2, 1.5,
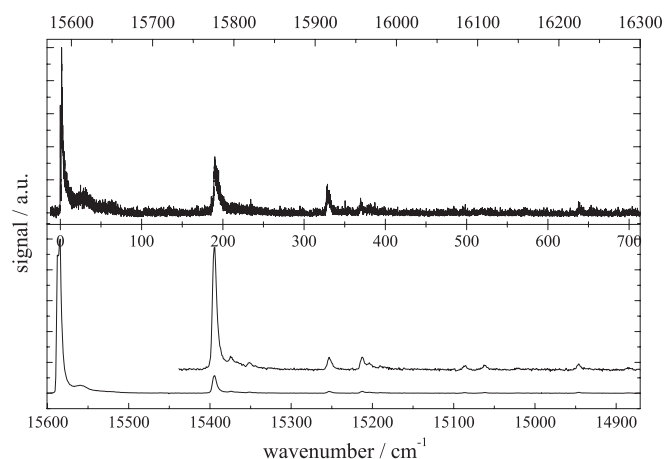

FIG. 6. (Top panel) Fluorescence excitation spectrum of TPC recorded by means of the pulsed setup. (Bottom panel) Dispersed emission spectrum of TPC recorded upon excitation at the electronic origin. The second trace is the same spectrum magnified by a factor of 7 in the intensity and shifted upwards.
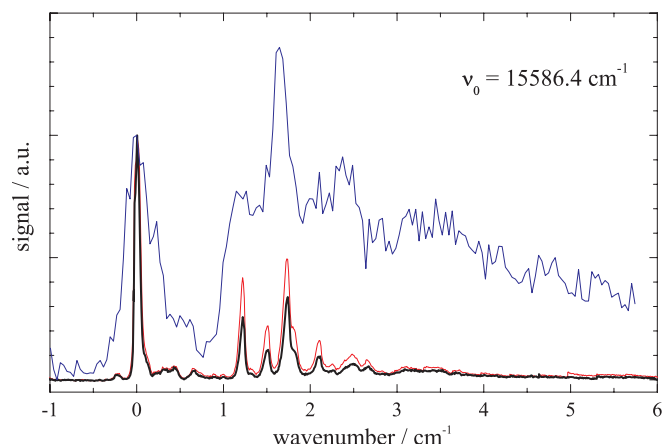

FIG. 7. Fluorescence excitation spectra of the electronic origin of TPC recorded with the cw setup at low (black line) and high (red line) laser intensity. The blue spectrum is taken from Fig. 6 and was recorded with the pulsed setup. The photon flux increases from black to red to blue. For details, see text.

1.7, 1.8, and 2.1 cm^{-1}. When using the pulsed setup (blue line), this fine structure reappears with increased line width and sitting partly on top of a broad PW. As revealed by variation of the laser intensity of the cw setup, this part of the signal exhibits a smaller oscillator strength as compared to the electronic origin. Moreover, dispersed emission upon excitation at any of the sharp peaks was coincident with the emission spectrum upon excitation at the first intense peak. Both observations favor an assignment of these sharp transitions to a second PW. A sharply structured PW may reveal the excitation of a non-superfluid helium solvation layer rigidly bound to the TPC molecule. It should be noted that these sharp spectral features beyond 1 cm^{-1} could alternatively be explained by the presence of different configurations of a TPC-helium solvation complex and, thus, represent the corresponding ZPLs. In this case, the redshifted emission might be due to relaxation into one global minimum configuration of the electronically excited system prior to radiative decay. Even if the experimental facts are not clearly exclusionary, in particular the saturation behavior favors an assignment to a PW.

IV. DISCUSSION

The present investigation of microsolvation in superfluid helium droplets by means of electronic spectroscopy profits mostly from careful consideration of the spectral resolution and by the comparative study of several related compounds. In particular, much care has been taken in studying the saturation behavior of the signals in order to avoid saturation broadening and to focus on the detection of ZPLs. Remarkable differences in the saturation behavior reveals different oscillator strengths which is an important criterion to distinguish between ZPL and PW. As shown in Fig. 4, the photon flux can substantially modify the spectral shape of electronic spectra. In the worst case, important structures of the spectrum remain hidden below an intense and spectrally broad PW. As already shown for tetracene, the fine structure of a ZPL may be smoothed out by saturation broadening.[13] The advantage of this experimental approach becomes evident in the reinvestigation of the electronic origin of porphyrin which shows the fully resolved triple peak feature for the first time (cf. Fig. 3).

In contrast to our previous comparative studies which we have done for anthracene derivatives or pyrromethene dye molecules,[3–7] for the porphyrin derivatives the low energy bending or torsional modes of the various substituents are absent in helium droplets. Thus, extended progressions possibly significantly broadened by the interaction with the helium environment were not observed. Moreover, porphyrin exhibits inversion symmetry and, thus, does not exhibit a permanent electric dipole moment. Depending on the configuration of individual substituents, the inversion symmetry may be lifted for the substituted compounds. Nevertheless, the electric dipole moment and its change upon electronic excitation is expected to be very small. Consequently, the two mechanisms identified as responsible for severe line broadening, namely, damping of large amplitude modes and drastic change of the electron density distribution, are absent for all

porphyrin compounds and also for TPC. Thus, the electronic spectra of the porphyrin derivatives showing exclusively very sharp ZPL peaks are in line with the empirical model proposed in Ref. 3.

With slight modifications, the triple peak feature resolved for porphyrin appears to be a fundamental spectral feature for all dopant species presented above. Therefore, we claim that this triple peak feature assigned as ZPL is the main spectral feature of the solvation of porphyrin derivatives in superfluid helium droplets. Most probable, this triple peak feature reveals three different configurations of a dopant helium solvation complex. The similarity and modifications of the triple peak feature observed for the seven dopant molecules can be seen as an expression of the porphyrin unit common to all compounds and the influence of the individual substituents, respectively. For DPP, the doublet of the triple peak feature may reveal two diastereomers which distinguish in the sense of the twist angle of the two phenyl moieties. In the case of TPP, the number of possible diastereomers with respect to the twist angel increases to four. The doubling of the TPP signal reveals the presence of only two diastereomers while the others are frozen out at a temperature of 0.37 K. For TPC, only a single triple peak feature is observed which speaks for the population of a single global minimum configuration possibly as a result of the reduced symmetry. For TMP and TPrP, the four ligands allow for numerous diastereomers. The number of possible diastereomers is expected to reach a maximum for the Etio compound. However, the low temperature conditions are effective on the corresponding population distribution. Thus, the number of triple peak features resolved in the spectra shown in Fig. 4 increases, however, not necessarily linearly with the number of possible diastereomers. The interpretation of our data remains highly empirical. The measurement of high resolution spectra taken in a supersonic molecular jet could provide additional information. All the helium-induced features such as triple peak and PW should be absent while the diastereomers of the substituted porphyrin compounds should be visible in the gas phase. However, such data as presented, for example, in Ref. 29 do not reach the spectral resolution necessary to resolve the multiplets observed in helium droplets. Moreover, the helium environment is known to stabilize metastable configurations[33] which might not be populated in the gas phase.

Only the low photon flux of the cw setup allowed us to record the origin of TPP in helium droplets. The assignment of the dominating signal was accomplished by a cross-check with the spectrum of a commercial TPC sample. Consequently, the spectrum reported in Ref. 30 for a commercial TPP sample is much likely that of TPC.[31] The first 400 cm^{-1} of the fluorescence excitation spectrum of helium droplets doped with a commercial sample of TPP by Callegari and Ernst[16] reveals the same peak positions as shown in the top panel of Fig. 6. The authors identify the electronic origin and two vibronic transitions which all couple to the progression of the torsional mode of the phenyl moieties. However, in the corresponding gas phase experiment,[29,30] the torsional wavenumbers are significantly smaller than in helium droplets (18 cm^{-1} versus 26 cm^{-1}). Together with the typical saturation behavior, we assign the 26 and 60 cm^{-1} peaks to

a PW. Interestingly, in the dispersed emission spectrum, the electronic origin is accompanied by the same spectral feature (cf. Fig. 6), now extending to the red, while the first intense vibronic transition is accompanied by two tiny and rather sharp peaks, shifted by 21 ± 2 and 43 ± 2 cm^{-1} to the red. These tiny peaks fit surprisingly well to a peak identified as hot band of the torsional mode in the gas phase experiment which was shifted by 22 ± 2 cm^{-1} to the red.[30] Thus, much evidence is provided that in the electronic ground state the 191 cm^{-1} mode promotes coupling to the torsional modes. However, an assignment of the two peaks at 212 and 234 cm^{-1} to different weak vibronic transitions of porphyrin cannot be excluded. In contrast, we assign the redshifted signal accompanying the electronic origin in the emission spectrum to a PW because of the close similarity of the spectral shape to the PW recorded in the excitation spectrum.

Finally, some remarks are needed on the experimental methods as well as on the reliability of the interpretation of the experimental data, because it is essential for the progress in deciphering the signature of microsolvation of molecules in superfluid helium nanodroplets. According to the generally accepted empirical model of solvation of molecules in helium droplets, one has to expect the following contributions in electronic spectra. First, there are pure molecular transitions assigned as ZPL which are expected to exhibit sharp transitions. Second, there is a PW which represents the excitation of the helium environment coupled to the molecular excitation. In many cases, the molecule is covered by a helium solvation layer consisting of a limited number of helium atoms localized on the surface of the molecule. Such a cluster is usually called solvation complex. The layer may exhibit its own excitation spectrum which appears as an additional contribution to the PW. Moreover, the solvation layer may exhibit different configurations each with its own solvent shift of the ZPL. Thus, the PW may carry additional spectrally rather sharp contributions while the ZPL may split up into a fine structure. In order to rationalize an assignment of the various spectral features to either a ZPL, a ZPL with fine structure, a PW, or a PW with fine structure we have studied the saturation behavior and the dispersed emission upon excitation at individual spectral positions. Generally, a ZPL shows strong saturation at high photon flux while the dispersed emission upon excitation at a PW appears redshifted. However, the observation of exclusively redshifted emission does not unequivocally prove for a PW and the degree of saturation does not necessarily correlate to ZPL and PW. As for ordinary Franck-Condon factors, a disadvantageous change of the equilibrium nuclear configuration may reduce the transition probability and, thus, the saturation even for a ZPL. Furthermore, the relaxation of the configuration of the helium solvation complex upon electronic excitation may cause a redshift in the corresponding emission. As mentioned already in Sec. III, alternative interpretations cannot be excluded for some of the experimental data. Therefore, we avoid to present a table listing the various assignments and attributions to each of the recorded signals. Instead, the final conclusion of this investigation is to declare the so called triple peak feature as the characteristic signature of the solvation of porphyrin derivatives in helium droplets whereas for all other details, the most probable of

various options have been identified, however, in several cases not exclusionary. We hope for a prolific reception by those who work on the theoretical part of microsolvation in helium droplets.

[1]M. Hartmann, R. E. Miller, J. P. Toennies, and A. F. Vilesov, Phys. Rev. Lett. **75**, 1566 (1995).

[2]R. Lehnig, D. Pentlehner, A. Vdovin, and A. Slenczka, J. Chem. Phys. **131**, 194307 (2009).

[3]D. Pentlehner, R. Riechers, A. Vdovin, G. M. Pötzl, and A. Slenczka, J. Phys. Chem. A **115**, 7034 (2011).

[4]D. Pentlehner, Ch. Greil, B. Dick, and A. Slenczka, J. Chem. Phys. **133**, 114505 (2010).

[5]D. Pentlehner and A. Slenczka, Mol. Phys. **110**, 1933 (2012).

[6]A. Stromeck-Faderl, D. Pentlehner, U. Kensy, and B. Dick, ChemPhysChem **12**, 1969 (2011).

[7]D. Pentlehner and A. Slenczka, J. Chem. Phys. **138**, 024313 (2013).

[8]M. Hartmann, A. Lindinger, J. P. Toennies, and A. F. Vilesov, Chem. Phys. **239**, 139 (1998).

[9]M. Hartmann, A. Lindinger, J. P. Toennies, and A. F. Vilesov, Phys. Chem. Chem. Phys. **4**, 4839 (2002).

[10]M. Hartmann, A. Lindinger, J. P. Toennies, and A. F. Vilesov, J. Chem. Phys. **105**, 6369 (2001).

[11]R. Lehnig and A. Slenczka, J. Chem. Phys. **122**, 244317 (2005).

[12]N. Pörtner, A. Vilesov, and M. Havenith, Chem. Phys. Lett. **368**, 458 (2003).

[13]N. Pörtner, J. P. Toennies, A. Vilesov, and F. Stienkemeier, Mol. Phys. **110**, 1767 (2012).

[14]J. P. Toennies and A. F. Vilesov, Angew. Chem. **116**, 2674 (2004); Angew. Chem., Int. Ed. **43**, 2622 (2004).

[15]F. Stienkemeier and K. K. Lehmann, J. Phys. B **39**, R127 (2006).

[16]C. Callegari and W. E. Ernst, "Helium droplets as nanocryostats for molecular spectroscopy from the vacuum ultraviolet to the microwave regime," in *Handbook of High-resolution Spectroscopy*, edited by M. Quack and F. Merkt (John Wiley & Sons, 2011), p. 1569.

[17]H. D. Whitley, J. L. DuBois, and K. B. Whaley, J. Phys. Chem. A **115**, 7220 (2011).

[18]H. D. Whitley, J. L. DuBois, and K. B. Whaley, J. Chem. Phys. **131**, 124514 (2009).

[19]H. D. Whitley, P. Huang, Y. Kwon, and K. B. Whaley, J. Chem. Phys. **123**, 054307 (2005).

[20]J. P. Toennies and A. F. Vilesov, Annu. Rev. Phys. Chem. **49**, 1 (1998).

[21]U. Even, J. Jortner, D. Noy, N. Lavie, and C. Cossart-Magos, J. Chem. Phys. **112**, 8068 (2000).

[22]D. Pentlehner, R. Riechers, B. Dick, A. Slenczka, U. Even, N. Lavie, R. Brown, and K. Luria, Rev. Sci. Instrum. **80**, 043302 (2009).

[23]M. Lewerenz, B. Schilling, and J. P. Toennies, Chem. Phys. Lett. **206**, 381 (1993).

[24]P. G. Seybold and M. Gouterman, J. Mol. Spectrosc. **31**, 1 (1969).

[25]R. Ballardini, B. Colonna, M. T. Gandolfi, S. A. Kalovidouris, L. Orzel, F. M. Raymo, and J. F. Stoddart, Eur. J. Org. Chem. **2003**, 288 (2003).

[26]P. P. Kumar and B. G. Maiya, New J. Chem. **27**, 619 (2003).

[27]M. Gouterman and G. E. Khalil, J. Mol. Spectrosc. **53**, 88 (1974).

[28]M.-C. Desroches, S. Layac, P. Prognon, P. Maillard, D. S. Grierson, E. Curis, I. Nicolis, and A. Kasselouri, Appl. Spectrosc. **57**, 950 (2003).

[29]U. Even and J. Jortner, J. Chem. Phys. **77**, 4391 (1982).

[30]U. Even, J. Magen, J. Jortner, J. Friedman, and H. Levanon, J. Chem. Phys. **77**, 4374 (1982).

[31]The first author of Ref. 30 agrees that his data may refer to TPC instead of TPP. The data have been obtained from a commercial sample used without further purification, private communication (2013).

[32]A. Lindinger, E. Lugovoj, J. P. Toennies, and A. F. Vilesov, Z. Phys. Chem. **215**, 401 (2001).

[33]M. Y. Choi, G. E. Douberly, T. M. Falconer, W. K. Lewis, C. M. Lindsay, J. M. Merritt, P. L. Stiles, and R. E. Miller, Int. Rev. Phys. Chem. **25**, 15 (2006).